

# Thermal performance of the ground in geothermal pavements

Yaser Motamedi<sup>1</sup>, Nikolas Makasis<sup>1</sup>, Arul Arulrajah<sup>2</sup>, Suksun Horpibulsuk<sup>3</sup>, Guillermo Narsilio<sup>1,\*</sup>

<sup>1</sup>Department of Infrastructure Engineering, University of Melbourne, Parkville, Australia

<sup>2</sup>Swinburne University of Technology, Melbourne, Australia

<sup>3</sup>School of Civil Engineering and Center of Innovation in Sustainable Infrastructure Development, Suranaree University of Technology, Nakhon Ratchasima, Thailand

**Abstract.** Shallow geothermal energy utilises the ground at relatively shallow depths as a heat source or sink to efficiently heat and cool buildings. Geothermal pavement systems represent a novel concept where horizontal ground source heat pump systems (GSHP) are implemented in pavements instead of purpose-built trenches, thus reducing their capital costs. This paper presents a geothermal pavement system segment (20m × 10m) constructed and monitored in the city of Adelaide, Australia, as well as thermal response testing (TRT) results. Pipes have been installed in the pavement at 0.5 m depth, and several thermistors have been placed on the pipes and in the ground. A TRT has been performed with 6kW heating load to achieve an understanding of the thermal response of the system as well as to estimate the effective thermal conductivity of the ground. The results show that the conventional semi-log method may be applicable to determine the thermal conductivity for geothermal pavements. The geothermal heat exchanger at shallow depth is considerably under the influence of the ambient temperature; however, it is still acceptable for exchanging the heat within the ground. It is also concluded that the impact radius of heat exchanger in geothermal pavement during the TRT is around 0.5m in the vertical and horizontal directions for this case study.

## 1 Introduction

Developing new technologies that can better utilise the benefits of renewable energy resources is increasingly attracting the attention of researchers worldwide, due to the increasing trends of greenhouse gas emissions and the urgent need for reversal of these trends [1]. Shallow geothermal energy is one such form of renewable energy, considered one of the more sustainable solutions that can aid towards providing future energy demands [2, 3]. This technology can be used to very efficiently provide thermal energy for space heating and cooling by utilising the ground as a heat source or heat sink [4, 5]. Heat is transferred to/from the ground via ground heat exchangers (GHEs), which comprise vertical or horizontal pipes in ground loops that circulate a carrier fluid. The GHEs are connected to a ground source heat pump (GSHP), which upgrades and transfers the heat to/from the building [6]. GSHP systems produce 4-5kW of thermal energy for every 1kW of electricity needed to run the system, rendering their coefficients of performance higher than conventional systems. Moreover, unlike other types of renewable energies, geothermal energy is always available [7] since these systems do not depend on the weather conditions. Even though the advantages of GSHP systems are remarkable,

the high capital costs associated with their installation can make it harder for these systems to be adopted more widely.

In addressing this issue, a more recent application of GSHP technologies relates to incorporating them early in the construction phase of a project, to take advantage of the construction earthworks and thus minimise the capital costs associated with building the GHEs. For example, energy piles have received significant attention over recent years, where HDPE pipes are implemented into foundation piles to also turn them to GHEs, instead of the traditional methodology which requires drilling purpose-built boreholes. The drawback of this approach, however, is that since the geothermal technology is installed based on existing construction plans and the geometry of the GHE is restricted by the structural design of the project, it can only provide a specified amount of thermal energy. Therefore, often hybrid systems are adopted, where GSHPs are used in conjunction with auxiliary means of thermal energy supply.

One application of GSHP technologies that has received very little attention thus far and is the focus of this study, relates to geothermal pavements. Geothermal pavements incorporate horizontal GHEs at a relatively shallow depth under the pavement (about 0.5 m depth,

\* Corresponding author: [narsilio@unimelb.edu.au](mailto:narsilio@unimelb.edu.au)

while the typical depth of horizontal GHE is 1 to 2 m), taking advantage of the existing required earthworks for road construction and thus significantly reducing the associated GSHP capital costs, such as for trenching. This can render GSHP systems cost-effective and can broaden their potential scope of application. Furthermore, geothermal pavements can easily be combined with other renewable sources, such as solar, to form a hybrid system and provide heating and cooling energy to nearby buildings.

The lack of available data on the potential of geothermal pavements makes it difficult for the technology to be adopted in the industry. One form of preliminary investigation that can provide an insight into the thermal behaviour of the system and ground is Thermal Response Testing (TRT). This is a standard in-situ test that circulates hot fluid in the GHEs and examines how well heat is transferred as well as identifies the thermal properties of the ground [8]. TRT testing has been primarily developed for vertical geothermal energy systems [9] and therefore most of the available TRT studies [10-12] investigate the performance of vertical geothermal energy systems with only a few studies covering the TRT in geothermal energy systems with Horizontal GHEs (HHEs). Fujii et al. (2010) performed a couple of TRTs on HHEs to compare the efficiency of horizontal and vertical slinky configurations [13]. By comparing the heat exchange rates and using the semi-log method to determine the thermal conductivity, it was concluded that the vertical slinky is more efficient. Phillipe et al. 2010 conducted four TRTs in four different HHEs under different ground surface conditions to study the soil temperature variations at horizontal and vertical distances of the HHE [14]. Another experimental study on TRT was performed by Yoon et al. 2015 to implement a cost-efficiency analysis between the slinky, spiral-coil and U-type HHEs. Results showed that the U-type HHE is the most efficient configuration technically and economically [5]. Kim et al. 2016 developed a numerical model in addition to the experiment to investigate the effect of HHE configuration and the thermal conductivity of the surrounding soil during a TRT test [3]. Fujii et al. 2019 ran a TRT in a horizontal trench with 8 m depth [15]. They assessed the heat exchangeability of the HHE and optimised the design parameters to increase the efficiency of the system as much as possible. The findings depicted that larger diameter and longer length of the pipes could obtain higher efficiency.

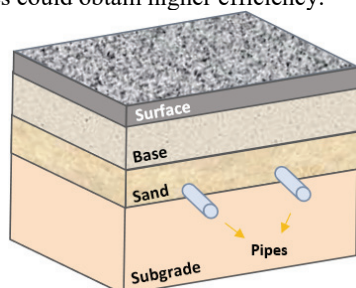


**Fig. 1.** Schematic of geothermal pavements (Not to scale)

Even though some investigations have been undertaken on TRTs in horizontal geothermal energy systems, there are still many gaps in our understanding of the thermal behaviour of the ground and the performance of horizontal GHEs, especially regarding geothermal pavements. This paper presents an experimental investigation of a pilot geothermal pavement system in a carpark located in Adelaide, specifically the City of Mitcham, in South Australia, including undertaking a TRT to further our understanding of its potential.

## 2 Experimental methodology

### 2.1 Geothermal pavements system

To investigate the thermal benefits of geothermal pavements, a carpark site was utilised, implementing the ground heat exchangers under the constructed pavement. The fieldwork activities commenced around February 2019, cooperating with the local parties and contractors and providing a suitable geothermal design. The geothermal pavement is implemented in a 200 m<sup>2</sup> (10 m×20 m) section of the carpark of, which had been excavated by 0.35 m, as required by the pavement construction, and only an additional 0.15 m of excavation was required to reach the designed 0.5 m GHE burial depth. As can be seen in **Fig. 1**, the pipes are located on the subgrade layer, however this can change for different projects, depending on the thickness and thermal properties of the relevant layers.

A total of 360 m of high-density polyethylene (HDPE) piping was laid at a depth of 0.5 m adopting a simple horizontal configuration and two circuits (only one of which is operated and analysed herein) as seen in **Fig. 2**.

The pipe spacing in each circuit is 0.6 m. The inner and outer diameter of pipes is 0.0201 m and 0.025 m, respectively. The pavement was designed to be able to provide up to about 4-5 kW energy, based on preliminary investigations and design guidelines on horizontal systems and has the potential to be connected to a nearby sports centre amongst others.

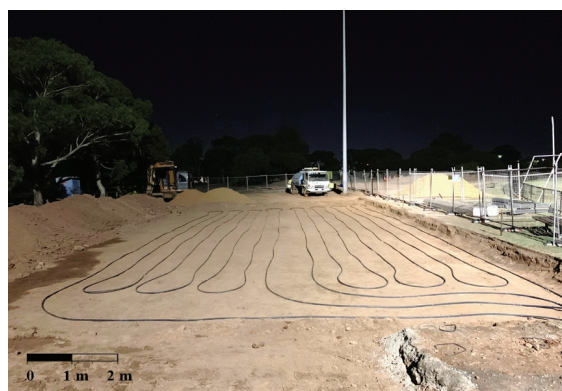


**Fig. 2.** Implementation of the geothermal pavements

### 2.2 Instrumentation

In order to obtain meaningful data from the experiment, detailed monitoring has been implemented on the site mainly including temperature sensors, shown in Figure Fig. 3. Tests were conducted only on one of the two HHEs circuits that form part of the pilot.

Firstly, sensors are placed at the inlet and outlet locations of the pipe loop to monitor the overall heat exchanged by its operation. Sensors 1, 2, 8 and 9 are installed on the subgrade layer attached on or near the pipes, providing insights on the heat transfer along the loop and along the horizontal deflection, while sensors 3, 4, 6 and 7 are installed within two 1 m deep backfilled boreholes to obtain the temperature 0.5 m and 1 m below the pipes (1 m and 1.5 m below the finished surface). After covering the pipes with a 0.2 m layer of fine sand, another set of sensors has been embedded at a depth of 0.3 m, labelled a1-a6 in Fig. 3. Overall, the large number of sensors incorporated can offer a clear picture of how the heat is transferred during the operation of the system.

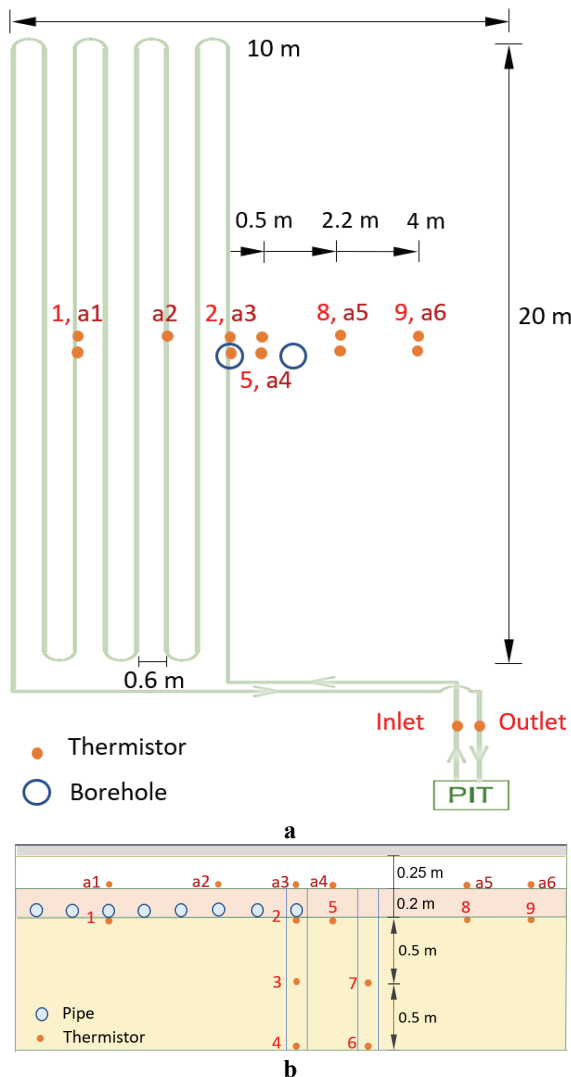


Fig. 3. Instrumentation of the pilot geothermal pavement: Top view (a) and side view (b). (Not to scale)

### 2.3 Field testing

A TRT was conducted in August 2018 for about 1.5 days, using a constant heat load of 6 kW. During the test, the flow rate was monitored by a flow meter and measured to be approximately constant at 0.28 L/s. Since one of the aims of the project is to see the thermal effect of the geothermal system to the surrounding environment/ground, the TRT was conducted on the first circuit which allowed the sensors of the second circuit to measure the ground temperature affected by the active circuit. Before the TRT testing, other in-situ tests; pressure test and flushing; have been undertaken on the site, to set up the test and provide suitable condition for testing, as shown in Fig. 4. In a pressure test, the pipes can be tested for strength and leaks. Flushing is also performed to eliminate the air bubbles and possible blocks inside the pipes. Furthermore, Since the ground thermal conductivity is a crucial parameter, needed for all analysis and modelling stages, thermal conductivity of different layers was measured using a handheld thermal needle probe equipment.

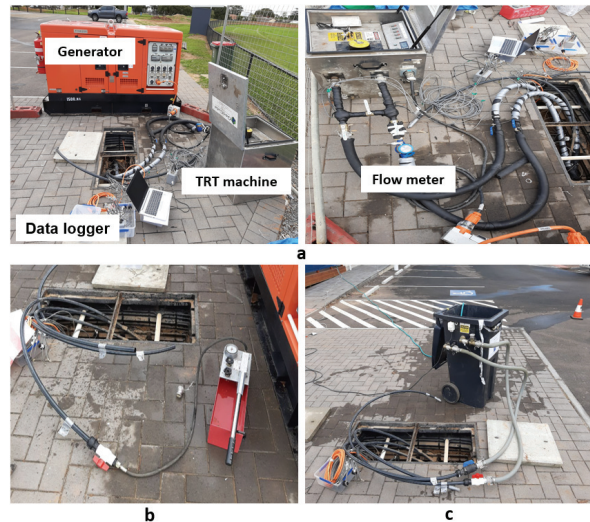


Fig. 4. Fieldwork: (a) TRT equipment, (b) Flushing, (c) Pressure test

### 2.4 TRT simplified analysis

The data from TRT are analysed to study the performance of the geothermal pavement system in terms of both the heat exchange rate as well as understanding the effect of the active heat exchanger on its surrounding media. The heat transfer process mainly involves conduction and convection, conduction being the dominant mechanism in the ground and pipe wall while convection in the carrier fluid. To calculate the heat exchange (in W) from the entire heat exchanger to its surroundings Equation 1 is used:

$$Q = m C \rho (T_{inlet} - T_{outlet}) \tag{1}$$

where m is the flow rate (in L/s), C is the heat capacity of water (4,186 J/kg/°C), ρ is its density (kg/m<sup>3</sup>) T<sub>Inlet</sub> and T<sub>Outlet</sub> are the temperature of the water in the inlet and outlet of the circuit (measured by sensors in °C).

TRTs are traditionally analysed by plotting the mean fluid temperature (average of inlet and outlet) against the logarithm of time and using equation 2 to estimate the thermal conductivity [16]. Even though this analysis relates to vertical borehole GHEs it is still considered valuable for comparison purposes.

$$Gradient = 2.303Q_1 / 4\pi\lambda \quad (2)$$

where the gradient is the slope of the plot in a logarithm cycle of time (usually the first cycle once the measurements reach steady state conditions),  $Q_1$  is the heat load per pipe length (W/m) and  $\lambda$  is thermal conductivity (W/m.K).

### 3 Results and discussion

#### 3.1 Inlet-outlet temperature and heat exchange

When performing a TRT, the temperature of the fluid at the inlet and outlet are analysed to evaluate how much heat was exchanged with the ground. These temperatures, as well as the ambient temperature of the environment are shown in **Fig. 5**. Overall, the trend is consistent with the literature showing a logarithmic growth, however, some anomalies exist in the data.

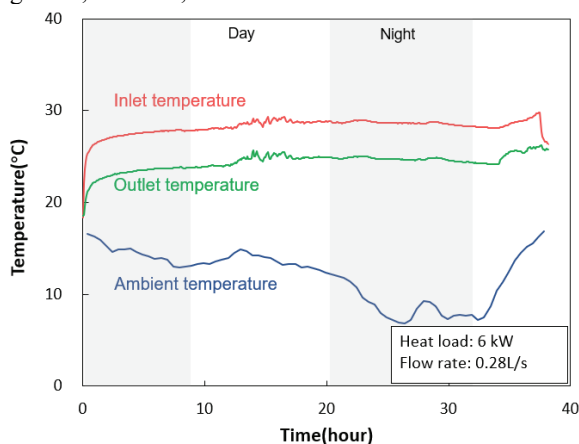


**Fig. 5.** Inlet and outlet temperature of the ground during the TRT, including ambient air temperature

Since the operational values such as flow rate and heat load are kept constant during the test, it is expected that this is the effect of climatic conditions (i.e. ambient temperature but also solar radiation). Observing the ambient temperature, it can be seen that the hotter the environment is (midday), the sharper the increase in the fluid temperature, which is most obvious in the second day (hours 34+) which was hotter. On the other hand, when it is cold outside (i.e. at night) a decline in the rise of the fluid temperature is observed, at times overtaking the heat injected to the ground, leading to an overall decrease of the fluid temperature (hours 25-30). The effect of the solar radiation is expected to not be negligible either, affecting both the TRT unit and the ground, however it was not measured in this study. One way to limit this influence can be to perform the TRT with a higher heat load, as is expected to decrease the

fluctuations of the inlet and outlet temperature. It is important to note that since the difference between inlet and outlet temperature is going to be used in determining the thermal conductivity, it is important to be confident in the utilised values and their consistency.

The heat exchange rate (per hour) between the GHE and the ground is also worth examining to understand how well the heat is transferred. **Fig 6** indicates the designed and real-time heat exchange rate for the test. While the TRT unit was adjusted to provide 6 kW heat load the real value was calculated as 4.52 kW by equation 1 using the measured flow rate of 0.28 L/s and the specific heat capacity of water that is 4,186 J/kg/°C.

The results suggest that 25% of the heat is lost in the TRT unit, hoses and pipes, which is consistent with the literature, stating values between 20%-25%. Calculating the (real) heat exchange rate per length of the pipe results in 25 W/m which comprises an acceptable heat transfer exchange rate for heating and cooling demands. It is also worth noting that the effect of ambient temperature on the TRT results is also evident here, with unstable heat exchange rates in midday, related to intense changes in ambient temperature and (presumably) solar radiation.

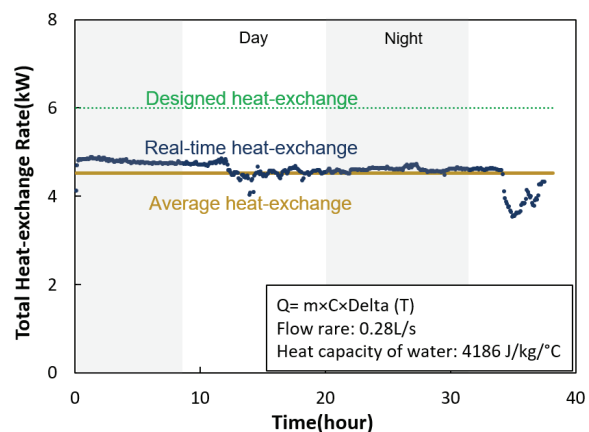


**Fig. 6.** Comparison of the designed and real-time heat exchange in the TRT.

#### 3.2 Thermal conductivity

To obtain the thermal conductivity, the conventional semi-log graphical method is used. Although the method was developed based on the line source theory for vertical heat exchangers, applying it to horizontal heat exchangers can serve as a comparison. **Fig. 7** shows the mean temperature of the inlet and outlet plotted against the time in logarithmic (log10) scale. Based on the literature [16], Equation 2 is only valid for times greater than a particular value which is 23,000 sec in this case. Therefore, the portion between 23,000 sec and 100,000 sec in the graph is utilised to calculate the gradient and thermal conductivity. Obtaining the gradient of the graph (2.3) and the real heat exchange rate (4.52 kW), the thermal conductivity in the test is then calculated as 2 W/m.K. Utilising the thermal needle probe equipment, the average thermal conductivity was measured as 1.7±0.2 W/m.K in ten different locations. Since the two

values are reasonably close, this suggests the potential applicability of this method for horizontal HHE TRT analysis. It is likely that the assumption of the circuit as a line by the theory, which is not correct for HHE, causes an overestimation of the value. Moreover, a high level of heat loss due to the very shallow depth of heat exchanger could be another cause of overestimation.

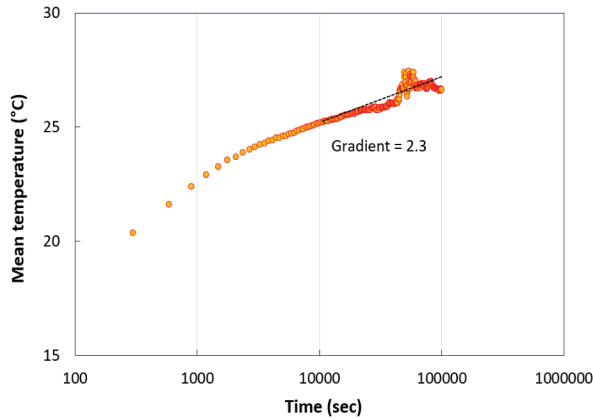


Fig. 7. Average fluid temperature vs. time in a logarithm scale.

### 3.3 Area of influence

This section investigates the effect of the active heat exchanger on the surrounding media. To do this, the distance, both horizontally and vertically, at which the ground temperatures are affected by the GHE operation needs to be identified. The effect of ambient temperature also needs to be considered, by using control points between the multiple sensors installed.

Fig. 8 depicts the measured temperature at varying depths of the ground during different times of the TRT (for labelling please see Fig. 3). As expected, near the surface the effect of the ambient temperature is obvious with large variations in temperature (ambient temperature varying between 7 to 15 °C).

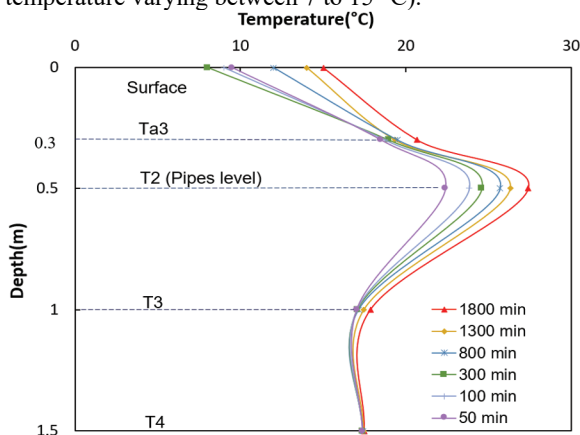


Fig. 8. Temperature of different depths of the ground at various time points after the start of TRT.

By increasing the depth, the temperature becomes more stable except for the depth of 0.5 m which is caused by the presence of geothermal pipes. All plots of different time points almost converge at a depth of 1 m with 16 °C indicating the maximum radius of influence

of heat exchanger in the vertical direction is around 0.5 m away from the pipes.

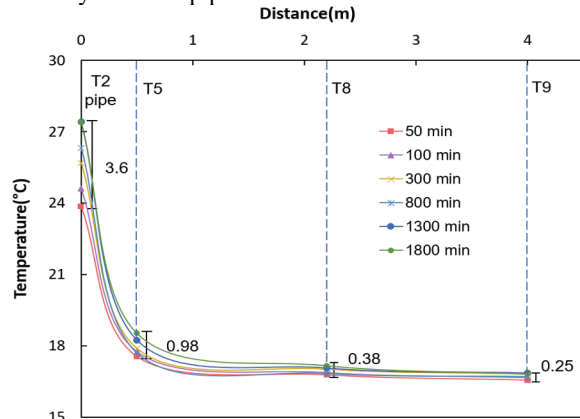


Fig. 9. Temperature of the ground in horizontal distances from the sensor T2 at various time points.

Similarly, the thermal effect in the horizontal direction is shown in Fig. 9. The origin point is sensor T2 which is connected to the pipe and represents the heat exchanger operation. Other sensors are installed at the horizontal distance of 0.5 m, 2.2 m and 4 m away from T2 (for labelling please see Fig. 3). Based on the figure, the temperature of the time points dramatically decreases from T2 to T5 while the temperature is relatively stable beyond the T5. On the other hand, the temperature variation range is meaningfully different between T2 and other spots. Therefore, the horizontal influence is considered about 0.55 m.

Considering both directions, the results suggest that the area of influence is about 0.5 m. This area is considered equal for both directions, despite the slight difference in value, since the shallow embedment depth of the pipes in geothermal pavements might be the reason the horizontal heat transfer is slightly more than the vertical.

## 4 Conclusion

A TRT has been performed in a real monitored geothermal pavement section to collect data and get a better understanding of the thermal conductivity, the effect of ambient temperature and heat transfer within the ground. The results showed that:

- 1- The conventional semi-log method which has originally developed for vertical systems may be applicable for horizontal heat exchanger in geothermal pavement. In this case study, it overestimates the thermal conductivity, however, the value is close to that of point measurements with the needle probe.
- 2- While the geothermal pavement is considerably under the influence of the ambient temperature; it still shows an acceptable heat exchange rate to exchange the heat to/from the ground.
- 3- For the particular geothermal pavement case, the radius of influence of the active heat exchanger is around 0.5 m. It should be noted that the soils used,

pavement structural package and operational condition influence this value.

By taking all aforementioned points into account, it can be concluded that geothermal pavements provide an opportunity to use the construction of pavements to install the heat exchanger at a lower cost compared to traditional systems, and therefore provide clean and renewable energy for heating and cooling buildings using a GSHP system.

Funding from the Australian Research Council (ARC) (project number LP170100072) and the University of Melbourne is much appreciated. Moreover, the third and fourth authors would also like to acknowledge the support from the National Science and Technology Development Agency (NSTDA), Thailand, under Chair Professor program (P-19-52303).

## References

1. Saha, D., et al., *CO2 capture in lignin-derived and nitrogen-doped hierarchical porous carbons*. Carbon, 2017. **121**: p. 257-266.
2. Narsilio, G.A. and L. Aye, *Shallow Geothermal Energy: An Emerging Technology*, in *Low Carbon Energy Supply*. 2018, Springer. p. 387-411.
3. Kim, M.-J., et al., *Thermal performance evaluation and parametric study of a horizontal ground heat exchanger*. Geothermics, 2016. **60**: p. 134-143.
4. Johnston, I., G. Narsilio, and S. Colls, *Emerging geothermal energy technologies*. KSCE Journal of Civil Engineering, 2011. **15**(4): p. 643-653.
5. Yoon, S., S.-R. Lee, and G.-H. Go, *Evaluation of thermal efficiency in different types of horizontal ground heat exchangers*. Energy and Buildings, 2015. **105**: p. 100-105.
6. Makasis, N., *Further understanding ground source heat pump system design using finite element methods and machine learning techniques*. 2018.
7. Schultz, A. and R. Petchey, *Energy update 2011*. Australian Bureau of Agricultural and Resource Economics and Sciences, Canberra, June, 2011.
8. Sanner, B., et al. *Thermal response test—current status and world-wide application*. in *Proceedings world geothermal congress*. 2005. International Geothermal Association.
9. Esen, H., M. Inalli, and M. Esen, *Numerical and experimental analysis of a horizontal ground-coupled heat pump system*. Building and environment, 2007. **42**(3): p. 1126-1134.
10. Makasis, N., et al., *Carrier fluid temperature data in vertical ground heat exchangers with a varying pipe separation*. Data in brief, 2018. **18**: p. 1466-1470.
11. Zarrella, A., et al., *Thermal response testing results of different types of borehole heat exchangers: An analysis and comparison of interpretation methods*. Energies, 2017. **10**(6): p. 801.
12. Chang, K.S. and M.J. Kim, *Analysis and thermal response test for vertical ground heat exchanger with two U-loop configuration*. International Journal of Energy Research, 2016. **40**(2): p. 189-197.
13. Fujii, H., et al. *Field tests of horizontal ground heat exchangers*. in *4th World Geothermal Congress*. 2010.
14. Philippe, M., et al. *An evaluation of ground thermal properties measure accuracy by thermal response test of horizontal ground heat exchangers*. 2010.
15. Fujii, H., et al. *Field Test of Horizontal Ground Heat Exchangers Installed Using Horizontal Directional Drilling Technology*. in *44th Workshop on Geothermal Reservoir Engineering*. 2019.
16. Banks, D., *An introduction to thermogeology: ground source heating and cooling*. 2012: John Wiley & Sons.